



## UNITED STATES AIR FORCE RESEARCH LABORATORY

### ANALYSIS OF CARDLAB DATA FOR INTERPUPILLARY AND VERTEX DISTANCE: NOTES ON THE CONSTRUCTION OF AN "EYE-BOX"

Elmar T. Schmeisser  
Dennis A. Maier

TASC  
4241 Woodcock Drive, Suite B-100  
San Antonio TX 78228-1330

July 1998

19980930 015

DDO QUALITY INSPECTED 1

*Approved for public release; distribution is unlimited.*

Human Effectiveness Directorate  
Directed Energy Bioeffects Division  
Optical Radiation Branch  
8111 18th Street  
Brooks Air Force Base TX 78235-5215

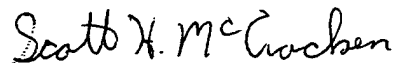
## NOTICES

This report is published in the interest of scientific and technical information exchange and does not constitute approval or disapproval of its ideas or findings.

Using Government drawings, specifications, or other data included in this document for any purpose other than Government procurement does not in any way obligate the US Government. The fact that the Government formulated or supplied the drawings, specifications, or other data does not license the holder or any other person or corporation; or convey any rights or permission to manufacture, use, or sell any patented invention that may relate to them.

The Office of Public Affairs has reviewed this technical report, and it is releasable to the National Technical Information Service, where it will be available to the general public, including foreign nationals.

This technical report has been reviewed and is approved for publication.



SCOTT H. MCCRACKEN, Captain, USAF  
Contract Monitor



RICHARD L. MILLER, PhD  
Chief, Directed Energy Bioeffects Division

REPORT DOCUMENTATION PAGE			Form Approved OMB No. 0704-0188	
Public reporting burden for this collection of information is estimated to average 1 hour per response, including the time for reviewing instructions, searching existing data sources, gathering and maintaining the data needed, and completing and reviewing the collection of information. Send comments regarding this burden estimate or any other aspect of this collection of information, including suggestions for reducing this burden, to Washington Headquarters Services, Directorate for Information Operations and Reports, 1215 Jefferson Davis Highway, Suite 1204, Arlington, VA 22202-4302, and to the Office of Management and Budget, Paperwork Reduction Project (0704-0188), Washington, DC 20503.				
1. AGENCY USE ONLY (Leave blank)		2. REPORT DATE July 1998		3. REPORT TYPE AND DATES COVERED Final Report - August 1997 - February 1998
4. TITLE AND SUBTITLE Analysis of CARDlab Data for Interpupillary and Vertex Distance: Notes on the Construction of an "Eye-box"			5. FUNDING NUMBERS C - F41624-97-D-9000 PE - 62202F PR - 7757 TA - 02 WU - 99	
6. AUTHOR(S) Elmar T. Schmeisser Dennis A. Maier				
7. PERFORMING ORGANIZATION NAME(S) AND ADDRESS(ES) TASC 4241 Woodcock Drive, Suite B-100 San Antonio TX 78228-1330			8. PERFORMING ORGANIZATION REPORT NUMBER	
9. SPONSORING/MONITORING AGENCY NAME(S) AND ADDRESS(ES) Human Effectiveness Directorate Directed Energy Bioeffects Division Optical Radiation Branch 8111 18th Street Brooks Air Force Base TX 78235-5215			10. SPONSORING/MONITORING AGENCY REPORT NUMBER  AFRL-HE-BR-TR-1998-0047	
11. SUPPLEMENTARY NOTES  Air Force Research Laboratory Technical Monitor: Captain Scott H. McCracken, (210) 536-6556.				
12a. DISTRIBUTION/AVAILABILITY STATEMENT  Approved for public release; distribution is unlimited.			12b. DISTRIBUTION CODE	
13. ABSTRACT (Maximum 200 words)  Data was obtained from the Wright-Patterson Air Force Base Computerized Anthropometric Research and Design lab (CARDlab) describing the quantitative three dimensional location of various facial landmarks. This data was compared to a set of similar measurements made in clinical optometric practice. The values obtained were analyzed for their statistical distribution. These values can be used to predict the fit of eye centered protective eyeware designs.				
14. SUBJECT TERMS Landmarks Protective eyeware			15. NUMBER OF PAGES 22	
			16. PRICE CODE	
17. SECURITY CLASSIFICATION OF REPORT Unclassified	18. SECURITY CLASSIFICATION OF THIS PAGE Unclassified	19. SECURITY CLASSIFICATION OF ABSTRACT -Unclassified	20. LIMITATION OF ABSTRACT  UL	

## CONTENTS

INTRODUCTION .....	1
DATA ANALYSIS.....	1
RESULTS FOR INTERPUPILLARY DISTANCE AND VERTEX DISTANCE.....	3
RESULTS: CONSTRUCTION OF THE EYEBOX.....	9
RESULTS: FOR VERTEX ADVANCE IN NON-IDEAL FITS.....	10
SUMMARY AND CONCLUSIONS .....	13
REFERENCES .....	13

## FIGURES

Figure No.

1 INDIVIDUAL DISTRIBUTIONS OF THE DATA.....	3
2 OVERLAPPED PLOTS OF THE MEASUREMENT DISTRIBUTIONS.....	4
3 PLOTTED DISTRIBUTIONS OF THE MEASURES .....	8
4 DISTRIBUTION OF 50% VERTICAL NOSE HEIGHTS.....	11
5 DISTRIBUTION OF 50% VERTEX ADVANCES.....	12

## TABLES

Table No.

1 LANDMARKS USED FOR CALCULATION.....	2
2 DESCRIPTIVE STATISTICS FOR THE DATA DISTRIBUTIONS.....	5
3 DESCRIPTIVE STATISTICS AFTER TRANSFORMATION .....	6
4 VERTEX DISTANCE DATA.....	7
5 INTERPUPILLARY DISTANCES.....	7
6 NUMERIC MEASURES OF THE 50% NOSE HEIGHT .....	11
7 NUMERIC MEASURES FOR 50% VERTEX ADVANCE .....	12

## INTRODUCTION

With the development of reflective filters using dielectric stack coatings on eyewear, the angular dependence of the device has become a design criterion. To overcome this inherent optical constraint of dielectric stack technology, the layers can be varied to maintain rejection of a desired wavelength based on where on the device surface they are placed. To do this efficiently, one must center the design on the center of rotation of the eye – thus producing an “eye-centered” design. In order to accomplish such a design, one must know what the population of eye locations in the skull is, and what their normal variation is. In order to provide this data, the Wright-Patterson Air Force Base Computerized Anthropometric Research and Design lab (CARDlab) web site maintainers were queried for information on what data existed and in what format it was available. These data were obtained through the help of Mr. Dave Hoeflerlin and Drs. Kathleen Robinette and Susan Blackwell from <http://www.al.wpafb.af.mil/~cardlab>. For comparison, further data was obtained from Dr. Mike Morris (SOLA, Inc.) on 384 patients. These data were also analyzed.

## DATA ANALYSIS

The CARDlab maintains two types of data: actual 3-d scans of heads and associated landmark files that tabulate the computer generated coordinates of standard anatomical locations. This information is not a “database”, but rather a repository of relatively raw data sets. Landmark files for a sample collection of head scans taken from pilots were downloaded. The data files are not in standard data format, but rather are formatted in punched card image format, i.e. the data are defined by which print column they occur in and are not otherwise delimited. In these files, there are several landmarks of interest (see table 1).

A BASIC program was written to extract these data into a standard format that could be imported into a spreadsheet program for manipulation. Of the 182 data files, 152 files had complete and useable data. The coordinates of the landmarks are given in both cylindrical and Cartesian coordinates. However, the “0” points for these coordinates are not aligned with the subject's head. By plotting these landmarks in cylindrical coordinates, it becomes clear that the head is not perfectly centered into the scan cylinder. Additionally, there is occasionally some slight tilt (both pitch and roll) of the head as well as an approximately 111 degree yaw. While these offsets can be mathematically corrected, for the purposes of this study, it is unnecessary.

Nuchale	Back of the head
Pronasale,	Tip of the nose
Left Tragion,	Approx. over the opening of the left ear
Left Ectocanthus,	outer corner of the left eye
Left Pupil,	Selected from a front view
Left Endocanthus,	Inner corner of the eye
Sellion,	Bridge of the nose
Right Endocanthus,	Inner corner of the right eye
Right Pupil,	Selected from a front view
Right Ectocanthus,	Outer corner of the right eye
Right Tragion,	Approx. over the opening to the right ear

Table 1: Landmarks used for calculation of relative distances.

Three simplifying assumptions need to be made:

1. that the amount of tilt (back to front) and roll (side to side) of the head is insignificant on average,
2. that the computer selected pupil points are consistent, and
3. that the bridge of the nose ("sellion") is a good estimator in the saggital plane for the horizontal location of the spectacle optical zone.

These assumptions are critical, and the second in particular is questionable. The scans were created with a laser wavelength that the cornea is transparent to (probably the red line from helium neon) and so the "depth" into the head of the pupil point is undefined. The pupil is a "hole" in the scan surrounded by a partially reflective iris creating an optical bottom (via scattering and blur) that probably depends on iris color and whose location in the head depends on the scanner angle. Further, the scan resolution (each digital volume element or voxel edge length) is on the order of 1 to 1.5 mm, which is relatively coarse for this application. This means that the "pupil" cannot be located to any better resolution than a rectangular cube of 0.986 mm across, 1.563 mm in vertical extent and with an undefined depth.

Taking these assumptions into account, the inter-pupillary distance (IPD) was calculated in 2 ways: first by simply taking the scanner generated xyz location data triplets of each pupil and calculating the shortest straight line distance between them. The second method was to ignore the landmark latitude coordinate, effectively collapsing the scan cylinder into a polar plot viewing the head from above. The angle and radius coordinates of each pupil was taken and converted into Cartesian (xy plane) equivalents, and the straight line distance calculated. The latter method allowed a simple derivation of

the estimated average vertex distance to be determined by calculating the distance from the interpupillary midpoint to the location of the projected sellion.

## RESULTS FOR INTERPUPILLARY DISTANCE AND VERTEX DISTANCE

Distributions of these distances (IPD from the xyz data; IPD and vertex distance from the polar plots) were calculated. Inspection of the data shows a normal or log normal distribution across the population, possibly with overlapping multiple distributions (split peaks). For comparison, plots of data obtained from 384 patients by Dr. Mike Morris (personal communication, SOLA, Inc.) are also provided. The plots are reproduced below (figure 1).

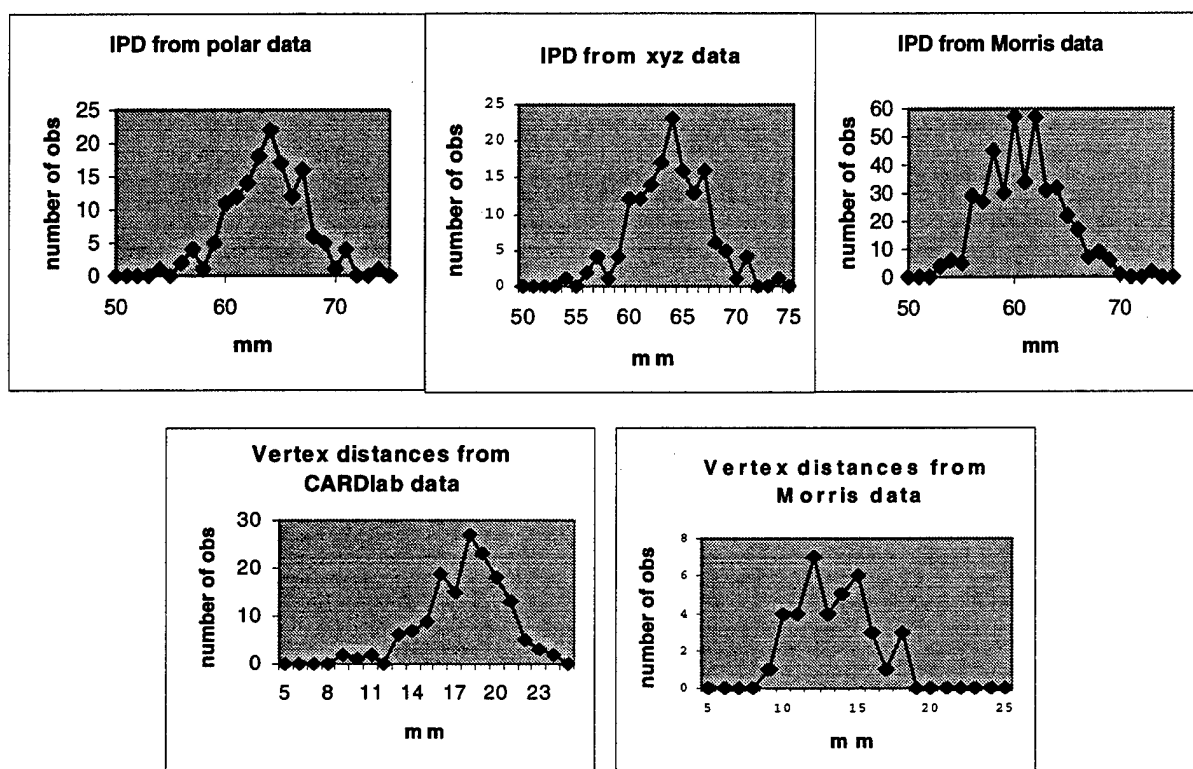


Figure 1: Individual distributions of the data observations for the five sets of measurements.

Overlapping these distributions after normalizing for the number of observations produces the following 2 plots for vertex and interpupillary distances, respectively (figure 2):

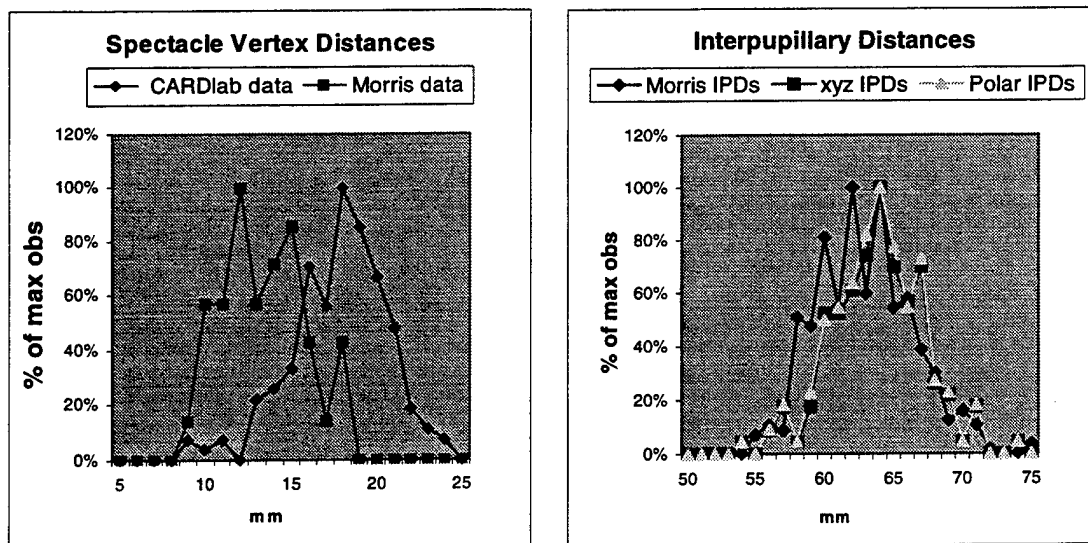


Figure 2: Overlapped plots of the measurement distributions from both the clinical and the CARDlab data sets.

As can be seen, the CARDlab data distributions differ from clinical, and the polar plot is very similar to the xyz plot. This is graphic confirmation that the assumptions of minimal tilt and roll of the head in the scan cylinder are valid. If there were any difference between the polar and xyz methods of calculating IPD from the CARDlab data, the polar method should foreshorten the distances compared to the xyz method.

Since the data theoretically is log-normally distributed, (i.e. the distances cannot decrease below zero), the sets were compared with a single factor ANOVA after log transformation. Surprisingly, the three IPD sets (M. Morris data, CARDlab polar and xyz derived data) were not significantly different ( $p=0.268$ ). Thus although the distributions appear to be different, their (logarithmic) means are sufficiently close and their variances sufficiently wide to be statistically indistinguishable by this parametric test. In contrast, the vertex distance data sets (M. Morris data vs. the CARDlab polar derived data) were separable ( $p<0.001$ ), reflecting the 4.3 mm difference in the average distance. This difference is probably due to the measurement, in that Dr. Morris' data is calculated from the cornea to the spectacle plane, while the CARDlab data is calculated from the pupil "bottom" to the sellion.



Submitting these data into Statistica (Statsoft, Tulsa, Ok) for distribution fitting and calculation of summary statistics resulted in the descriptions shown in table 2 for the raw data.

		MM_VERT	POLAR_VE	MM_IPD	POLAR_IP	XYZ_IPD
	Valid N	38	152	424	152	152
	mean	12.9079	17.3218	62.8290	63.3015	63.3491
Confid.	-95.000%	12.1034	16.8686	62.4950	62.7687	62.8160
Confid.	+95.000%	13.7123	17.7750	63.1630	63.8343	63.8822
	median	12.4750	17.6584	63.0000	63.4591	63.4683
	mode	multiple	no mode	64.0000	no mode	no mode
freq-cy	of mode			47.0000		
	minimum	8.3500	8.2400	55.0000	53.7853	53.8166
	maximum	18.0000	23.5486	75.0000	73.3436	73.4138
25.000th	percentl	11.0500	15.7408	60.0000	61.3714	61.3811
75.000th	percentl	14.9000	19.2633	65.0000	65.7680	65.7910
geometric	mean	12.6831	17.0651	62.7327	63.2142	63.2618
harmonic	mean	12.4606	16.7708	62.6371	63.1263	63.1738
	std.dev.	2.4474	2.8279	3.4989	3.3246	3.3264
	variance	5.9899	7.9972	12.2420	11.0532	11.0649
average	deviatn.	2.0557	2.1976	2.8180	2.5926	2.5933
	range	9.6500	15.3086	20.0000	19.5583	19.5972
Quartile	range	3.8500	3.5225	5.0000	4.3965	4.4099
	skewness	0.2806	-0.5784	0.3331	-0.0744	-0.0752
	kurtosis	-0.7240	0.6663	0.0177	0.3413	0.3354

Table 2: Descriptive statistics for the data distributions graphed in figures 1 and 2. MM-VERT is the vertex distance data from Dr. Morris; POLAR\_VE is the vertex distance calculated from the CARDlab data via the polar method; MM\_IPD is the interpupillary distance data from Dr. Morris; POLAR\_IP is the CARDLAB interpupillary distance via the polar method; XYZ-IPD is the interpupillary distance from the CARDlab data by the shortest straight line between the pupil landmarks).

Transforming the data into its logarithms and rerunning the summary statistics produced the following (table 3):

		LOGMM_VE	LOGPOLAR	LOGMM_IP	LOGPOLAR	LOG_XYZI
	Valid N	38	152	424	152	152
	mean	1.1032	1.2321	1.7975	1.8008	1.8011
Confid.	-95.000%	1.0760	1.2196	1.7952	1.7971	1.7975
Confid.	+95.000%	1.1304	1.2446	1.7998	1.8045	1.8048
	median	1.0960	1.2470	1.7993	1.8025	1.8026
	mode	multiple	no mode	1.8062	no mode	no mode
freq-cy	of mode			47.0000		
	minimum	0.9217	0.9159	1.7404	1.7307	1.7309
	maximum	1.2553	1.3720	1.8751	1.8654	1.8658
25.000th	percentile	1.0434	1.1970	1.7782	1.7880	1.7880
75.000th	percentile	1.1732	1.2847	1.8129	1.8180	1.8182
Geometric	mean	1.1002	1.2295	1.7973	1.8007	1.8010
Harmonic	mean	1.0971	1.2267	1.7972	1.8005	1.8009
	std.dev.	0.0827	0.0781	0.0241	0.0229	0.0229
	variance	0.0068	0.0061	0.0006	0.0005	0.0005
Average	deviation.	0.0694	0.0585	0.0195	0.0179	0.0179
	range	0.3336	0.4560	0.1347	0.1347	0.1349
Quartile	range	0.1298	0.0877	0.0348	0.0300	0.0301
	skewness	-0.0569	-1.2900	0.1797	-0.2564	-0.2566
	kurtosis	-0.7574	2.7513	-0.1417	0.4021	0.3968

Table 3: Descriptive statistics for the data after transformation to logarithms, in order to fit a normal distribution. Data is arranged in the same order as in Table 2.

This transformation produced a better fit to a normal distribution than with the linear data. The various boundary values can be calculated by back-transforming the metrics from the logarithmic form (i.e. linear data =  $10 \exp \log$  data). Thus the means and  $\pm 2$  S.D. limits of the M. Morris IPD log data set is 62.73 mm [56.14 mm - 70.10 mm]. Back transformation results in the following (tables 4 and 5):

		LOGMM_VE	LOGPOLAR	MMORRIS	CARDlab
	Valid N	38.	152.		
	mean	1.1032	1.2321	12.6831	17.0651
Confid.	-95.000%	1.0760	1.2196	11.9131	16.5805
Confid.	+95.000%	1.1304	1.2446	13.5028	17.5638
	median	1.0960	1.2470	12.4748	17.6584
	mode	Multiple	no mode		
	minimum	0.9217	0.9159	8.3500	8.2400
	maximum	1.2553	1.3720	18.0000	23.5486
25.000th	percentl	1.0434	1.1970	11.0500	15.7408
75.000th	percentl	1.1732	1.2847	14.9000	19.2632
geometric	mean	1.1002	1.2295	12.5945	16.9625
harmonic	mean	1.0971	1.2267	12.5059	16.8533
	std.dev.	0.0827	0.0781	1.2099	1.1969
	variance	0.0068	0.0061	1.0159	1.0141
average	deviatn.	0.0694	0.0585	1.1733	1.1443
	range	0.3336	0.4560	2.1557	2.8578
quartile	range	0.1298	0.0877	1.3484	1.2238
	skewness	-0.0569	-1.2900		
	kurtosis	-0.7574	2.7513		

Table 4: Vertex distance data. LOGMM\_VE and LOGPOLAR are the Morris and CARDlab data, respectively. The columns headed MMORRIS and CARDlab are these numbers retransformed from their logarithmic form into linear form.

		LOGMM_IP	LOGPOLAR	LOG_XYZ	MMORRIS	CARDlab/pol	CARDLAB/xyz
	Valid N	424.0000	152.0000	152.0000	424.0000	152.0000	152.0000
	mean	1.7975	1.8008	1.8011	62.7327	63.2142	63.2618
Confid.	-95.000%	1.7952	1.7971	1.7975	62.4019	62.6814	62.7286
Confid.	+95.000%	1.7998	1.8045	1.8048	63.0652	63.7516	63.7995
	median	1.7993	1.8025	1.8026	63.0000	63.4591	63.4683
	mode	1.8062	no mode	no mode			
	minimum	1.7404	1.7307	1.7309	55.0000	53.7853	53.8166
	maximum	1.8751	1.8654	1.8658	75.0000	73.3436	73.4138
25.000th	percentl	1.7782	1.7880	1.7880	60.0000	61.3714	61.3811
75.000th	percentl	1.8129	1.8180	1.8182	65.0000	65.7680	65.7910
geometric	mean	1.7973	1.8007	1.8010	62.7095	63.1931	63.2406
harmonic	mean	1.7972	1.8005	1.8009	62.6864	63.1718	63.2194
	std.dev.	0.0241	0.0229	0.0229	1.0569	1.0542	1.0542
	variance	0.0006	0.0005	0.0005	1.0013	1.0012	1.0012
average	deviatn.	0.0195	0.0179	0.0179	1.0458	1.0420	1.0420
	range	0.1347	0.1347	0.1349	1.3636	1.3636	1.3641
quartile	range	0.0348	0.0300	0.0301	1.0833	1.0716	1.0718
	skewness	0.1797	-0.2564	-0.2566			
	kurtosis	-0.1417	0.4021	0.3968			

Table 5: Interpupillary distances (Morris data, polar and xyz methods from the CARDlab data). Data arranged as in table 4.

Plotting both the linear and the logarithmic data as the appropriate box and whisker graphs (see legends) produces the following (figure 3):

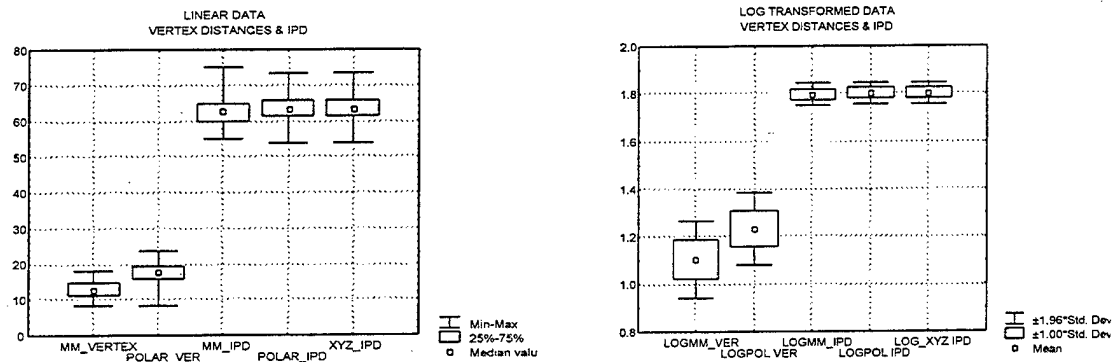


Figure 3: Plotted distributions of the measures (both linear and logoarithmic) for interpupillary distance and vertex distance from the two data sets described in the text.

The Army Optometry clinic at BAMC was contacted to determine if there existed a clinical database for vertex distances (personal communication: SFC Colon). According to the clinic guidelines, vertex distances are not routinely specified except for cataract patients who do not receive an intraocular lens implant. There is standard vertex distance guidance given of 10 – 12 mm for normal glasses. Searches of the Internet web space showed relatively few sites that had specifications for vertex distances (see for example: <http://www.direct.ca/excel/scuba>). These were also only planning distances ranging from 12 to 14 mm, with the occasional note that smaller is better (e.g. for corrections during visual field perimetry).

Summarizing the above, there seems to be enough data from both the CARDlab and from Dr. Morris to make some predictions about the distributions of interpupillary distances, and thus to support the calculation of a volume of space that encompassed the range of normal pupil excursions, i.e. an “eyebbox”. The distribution of vertex distances is marred in the CARDlab data by the indeterminacy of the pupil “depth” into the head, and in the clinical data by the variances in glasses frame styles, but may suffice for planning. A larger source of variation may arise from the slippage of the proposed spectacle frames on the face, resulting in a greater vertex distance than the design parameter (see below).

## RESULTS: CONSTRUCTION OF THE EYEBOX

Local reference databases were searched for papers that might address a mathematical model of eye movement. Such a model could allow a specification of the region of space swept out by the possible excursions of the pupil during normal pursuit eye movement.<sup>1</sup> Reviewing the academic literature shows that most of the models were oriented towards describing the movement and speed of the point of fixation in small angle saccades (e.g. less than 30 degrees), and did not address the full range of motion of the human eyeball.<sup>2,3,4</sup>

However, clinical estimates can be made of the relationship between angle of deviation and mm of pupil movement along the lid margin.<sup>5</sup> These relationships are 1 degree of deviation of the line of sight = 2 prism diopters and 1 mm of movement is approximately 5 degrees of deviation, or 10 prism diopters. These numbers provide the conversion factors needed to establish the physical range of pupil movement in the skull.

One simplifying assumption needs to be made: the range of pupil movement is to be restricted to the binocular visual field. This range is limited nasally by (of course) the nose. The extent of the nasal visual field is commonly taught as 60 degrees maximum.<sup>6</sup> Further, the binocular visual field is approximately circular. Since one can see one's own nose, the maximum excursion to be considered is 60 degrees.

With 60 degrees radius as a maximum, this implies a 120 degree field. This maximum results in 240 prism diopters, which equals 24 mm of excursion. This distance will define the vertical extent of the "eye-box" (defined as the volume of all possible pupil positions). The horizontal extent is defined by the IPD (mean=63 mm) plus these same 24 mm of excursion, which equals 87 mm.

The depth of the eye-box into the skull is set by the apparent regression of the pupil towards the back of the head in lateral gaze. Assuming a 25.4 mm diameter eye, the radius from the center of rotation of the eye is approximately 13 mm. Subtracting the anterior chamber depth of about 2 mm gives 11 mm. The regression will be  $11 \text{ mm} * (1 - \cos 30 \text{ deg}) = 1.47 \text{ mm}$ . Adding in the recession due to the apparent pupil radius (i.e. the resulting minor axis of the ellipse) of  $0.13 * 4 = 0.5 \text{ mm}$  results in 2 mm.

In summary, the maximum excursion of the pupil (the binocular eye box) is bounded by a rectangular solid 87 mm wide, by 24 mm tall by 2 mm deep. The actual positions swept out by the pupil itself will be a curved surface lying within this box.

To construct a monocular eye-box, defined as the rectangular solid encompassing the physical excursions of one pupil, several assumptions are needed (as before).

- a) The pupil's visibility will be restricted by the anatomical obstructions of the eyebrows, cheeks, and the nose. This limits the maximal eye-box to 60 degrees nasal, 60 degrees superior, and 75 degrees inferior to the visual axis.

- b) With an eye rotation of 60 degrees temporally, a maximally expanded temporal field of view of 155 degrees can result (60 degrees plus the 95 degrees of static temporal visual field).
- c) It is assumed that with a rotation of 30 degrees, a compensatory head turn will occur, limiting further rotation of the eye. Thus, the maximal lateral field of interest reduces to 125 degrees.
- d) The pupil diameter can be estimated (worst case) to be 8 mm.

The third assumption (c) provides the smallest potential volume for the pupil excursion. However, the peripheral retina still will be accessible through the pupil with off-axis exposures out to 95 degrees temporal to the line of sight. The most oblique rays are refracted into the pupil by passing through the tilted optics of the corneal margin. The eyeball radius is measured from the center of rotation to the plane of the pupil is assumed to be 11 mm (26 mm diameter / 2 – the anterior chamber depth of 2 mm). A 30 degree physical excursion results in a lateral shift of the pupil center by 5.5 mm ( $\sin 30^\circ \times 11$ ). Adding in the pupil radius (4 mm) results in a horizontal and vertical extent for this monocular eye-box of 9.5 mm. This calculation overestimates the pupil's contribution since its apparent size will decrease with rotation by 50% ( $\sin 30^\circ$ ). The corrected extent then becomes 7.5 mm.

The same 30 degree shift will result in an apparent pupil regression of 1.5 mm [ $(1 - \cos 30^\circ) \times 11$ ]. Adding in the recession due to the apparent pupil radius (i.e. the resulting minor axis of the ellipse) of  $0.13 \times 4 = 0.5$  mm produces a depth for the eye-box of 2.0 mm. In summary, the 30 degree monocular eye-box is bounded by a rectangular solid 7.5 by 7.5 by 2.0 mm centered on the forward line of sight and whose anterior surface is in the pupil (iris) plane of the eye.

## RESULTS FOR VERTEX ADVANCE IN NON-IDEAL FITS

Finally, the effects of slippage of the LEP down the nose should be considered. The CARDlab landmarks includes a point at the tip of the nose (pronasale), so that by calculating differences between sellion and this point, both the advance as well as the drop of the LEP can be estimated.

Plotting the distribution of the 50% "average" nose produces an approximately normal curve (figure 4). The expected drop in the eyewear center with a 50% slippage is about 2 cm (table 6).

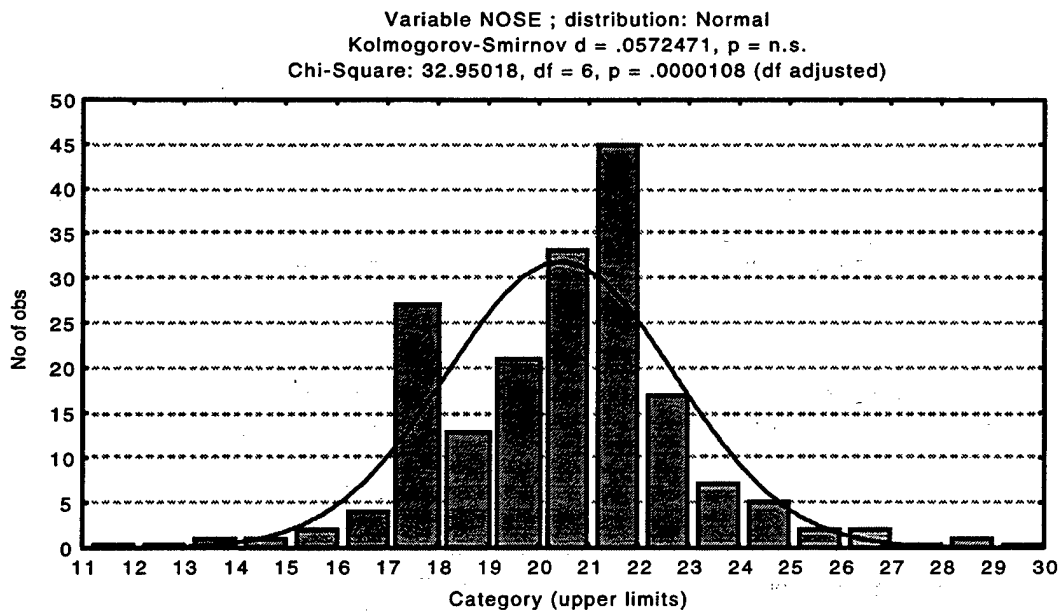


Figure 4: Distribution of 50% vertical nose heights, calculated from the difference between the CARDlab altitude figures between sellion and the tip of the nose.

	Valid N	181
	Mean	20.43558
Confid.	-95.000%	20.10305
Confid.	+95.000%	20.76811
	Median	20.319
	Mode	20.319
freq-cy	of mode	33
	minimum	13.2855
	maximum	28.134
25.000th	percentl	18.756
75.000th	percentl	21.882
geometric	mean	20.30827
harmonic	mean	20.17763
	std.dev.	2.267227
	variance	5.14032
average	deviatn.	1.746202
	range	14.8485
quartile	range	3.125999
	skewness	0.033688
	kurtosis	0.772763

Table 6: Numeric measures of the 50% nose height data distribution

The vertex advance is also approximately normally distributed with a mean of approx. 1 cm. (figure 5 and table 7).

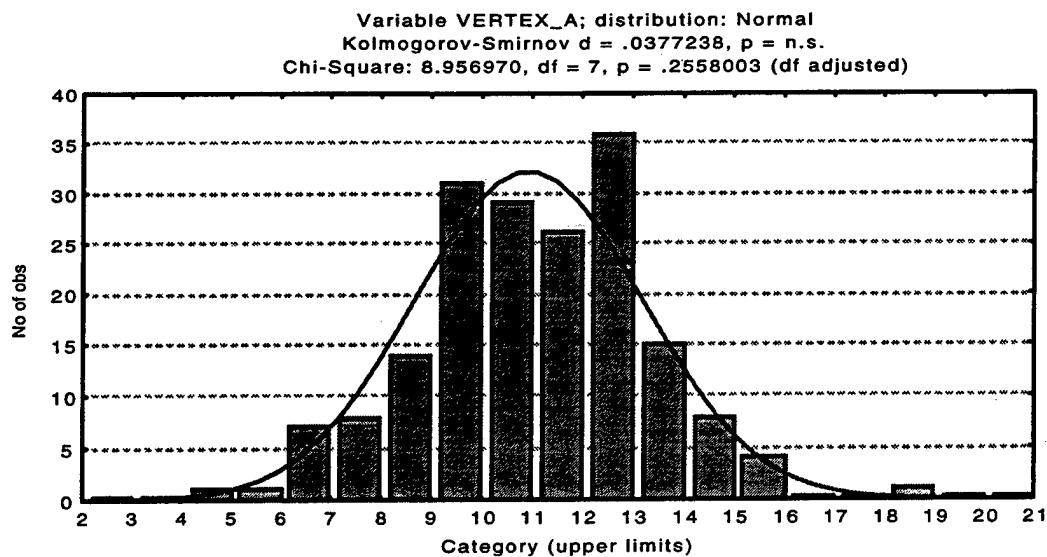


Figure 5: Distribution of 50% vertex advances calculated from the CARDlab radius data.

	valid N	181
	mean	10.92481
Confid.	-95.000%	10.59578
Confid.	+95.000%	11.25383
	median	10.965
	mode	12.515
freq-cy	of mode	3
	minimum	4.36
	maximum	18.905
25.000th	percentl	9.335
75.000th	percentl	12.36
geometrc	mean	10.67987
harmonic	mean	10.41094
	std.dev.	2.243324
	variance	5.032502
average	deviatn.	1.78705
	range	14.545
quartile	range	3.025
	skewness	-0.00201
	kurtosis	0.502901

Table 7: Numeric measures for 50% vertex advance.



## SUMMARY AND CONCLUSIONS

Distributions of the interpupillary distances and vertex distances have been derived. The final integrated volume needed for both binocular and monocular eye-centered designs has been determined. Predictions of the changes in vertex distance and eyebox center with non-ideal wearing conditions have been calculated. Further work will establish tradeoffs between protection and engineering feasibility in such designs with present technology.

## REFERENCES

1. Kosnik, W.D. (1988) A Preliminary Model Of The Distributions Of Laser-Induced Retinal Lesions Resulting From Eye And Head Responses. (USAFSAM-TR-88-19), Brooks Air Force Base, TX : USAF School of Aerospace Medicine, Human Systems Division (AFSC).
2. Epelboim, J., Kowler, E. (1993) Slow control with eccentric targets: Evidence against a position-corrective model. *Vision Research* 33:361-380.
3. Steinman, R.M., Kowler, E., Collewyn, H. (1990) New directions for oculomotor research. *Vision Research* 30:1845-1864.
4. Aslin, R.N., Shea, S.L. (1987) The amplitude and angle of saccades to double-step target displacements. *Vision Research* 27:1925-1942.
5. Wiener, A. (1940) *Surgery of the eye*, pp 355-356. Philadelphia:Saunders & Co.
6. Stein, H.A., Slatt, B.J. (1971) *The Ophthalmic Assistant*, pp. 205-206. St. Louis: Mosby Co.